Western Region Technical Attachment
NO. 04-08
August 3, 2004

A Procedure for Forecasting Dry Thunderstorms in the Great Basin using the Dynamic Tropopause and Alternate Tools for Assessing Instability

Jim Wallmann
NWSFO Reno, NV

1. Introduction

Forecasting "dry" thunderstorms (less than 2.5 mm or 0.10 inches rainfall for Nevada – other locations may have different criteria depending on the vegetation present) in the western United States has always been difficult. More importantly, dry thunderstorm events often lead to large wildfire outbreaks in this region. Some recent research (Rorig and Ferguson 1999; Rorig et al. 2003) has investigated the thermodynamic parameters involved with dry lightning outbreaks and the probability that thunderstorms will be dry. However, thermodynamic parameters alone are often not sufficient for outbreaks without forcing from an atmospheric disturbance. Pattern recognition, based on quasigeostrophic (QG) theory, is another commonly used tool available to forecasters in western United States forecast offices (NWS 1996). Alas, most of the patterns are only briefly described therein, and serve mainly as an introduction to observed dry lightning patterns. Recently, Nevada dry lightning outbreaks have been reinvestigated and placed into two main categories: dry thunderstorms from the advection of monsoon moisture, and those triggered by a negatively tilted short wave trough. This paper will analyze dry thunderstorm outbreaks associated with negatively tilted short wave troughs.

A few years ago, Gibson (1995 and 1996) illustrated the utility of isentropic potential vorticity (PV) (Hoskins et al. 1985) for forecasting convection and surface cold fronts in the western United States in summer, which often result in extreme fire behavior. This paper will use similar concepts to Gibson in diagnosing upper level fronts, but goes further by using the dynamic tropopause (DT). A review of the use of PV thinking in diagnosing upper level fronts and the motivation for using DT is describe in section 2. Section 3 will describe a procedure based on the DT to forecast dry thunderstorm development and discuss three additional methods of assessing atmospheric instability. The usefulness of the DT method is illustrated through a case study with potential model shortcomings in section 4. A brief summary and conclusions are presented in section 5.

2. Motivation for the Use of the Dynamic Tropopause

In illustrating the operational usefulness of upper level fronts through PV thinking, Gibson (1995 and 1996) used Ertel PV of a mean layer (as done in Shapiro and Grell 1994). Ertel PV, as shown in Holton (1992), is illustrated in the equation in isentropic coordinates:

$$PV \equiv (\zeta_\theta + f)(-g\frac{\partial\theta}{\partial p}) = const$$

where Ertel's PV is a product of absolute vorticity and the dry static stability that is conserved in adiabatic frictionless flow. Gibson used cross-sections of PV and potential temperature to show the movement and distribution of PV. Gibson noted that using a layer was not a favorable way to view Ertel PV in the upper troposphere and lower stratosphere since it is not conserved in an isobaric layer and therefore advection by the layer wind may give poor results. However, Gibson used layers due to the ease of computation in the NWS operational environment at the time. By using an isentropic surface, which is readily available in the Advanced Weather Interactive Processing System (AWIPS), Ertel PV advection can easily be deduced from the wind field as long as diabatic heating and/or cooling is not significant at the time and area of interest. However, the disadvantage of this method is that several isentropic surfaces are needed to get a full description of the PV distribution and advection. Instead, this discussion will use dynamic tropopause (DT) charts, usually calculated on the 1.5 or 2 Potential Vorticity Units (PVU – K kg^{-1} m^2 s^{-1}) isertelic surface (this paper will use the 1.5 PVU isertelic surface), which are common isertelic surfaces used in numerous studies (Hoskins and Berrisford 1988; Bosart and Lackmann 1995; Hakim et al. 1995; Bosart et al. 1996 are just a few).

The DT is used because it has the advantage that Ertel PV gradients are concentrated at the tropopause so a more three-dimensional view of PV distribution can be seen on a two-dimensional surface. In general, tropospheric air is lower in static stability so PV values are lower with high values of PV located in the stratosphere with its high static stability. Therefore, the DT is often considered a more robust method of determining the tropopause compared to the WMO definition based on lapse rates, because of the gradients in PV located near the tropopause. In addition, PV advection can easily be seen on only one chart in the absence of diabatic effects. However, it is important to note that only potential temperature is conserved on the DT, not pressure. (Some operational meteorologists may find it easier to use pressure in assessing the depth and slope of the DT.) In addition, the 'destruction' of PV due to diabatic heating on an isentropic surface can be visualized by the rise of the DT. The DT is also now available in AWIPS which makes it easier for the operational NWS forecaster to infer the three-dimensional distribution of PV on a two-dimensional chart.

3. Description of forecast tools

a) The dynamic tropopause

Advection of potential temperature (θ) and/or pressure on the DT is very useful in analyzing the location of an upper level front and the expected vertical motion. Using PV thinking (slightly different descriptions of PV thinking can be found in Hoskins et al. 1985; Hirschberg and Fristch 1991a,b; and Bluestein 1993), the higher-to-lower advection of pressure/θ on the DT can be used to infer forcing for upward vertical motion. Positive pressure advection on the DT is similar to positive PV advection on an

isentropic surface. (It is important to remember, however, that pressure is not a conserved quantity on the DT, but θ is.) Thus, the advection of PV can be used to assess one mechanism for upward vertical motion necessary for a convective outbreak. From now on, this paper will refer to positive DT pressure advection. In addition, use of the DT can show the return of PV to the stratospheric reservoir in a layer where convection is occurring as the DT rises in response. If this were to occur ahead of the upper level front, it would act frontogenetically and therefore strengthen the upper front with the associated lift stronger downstream.

An example of positive DT pressure advection from the 12 UTC RUC Analysis for 22 Jul 2002 is given in Figure 1. In the left panel, only the DT pressure and winds are shown and it is apparent positive pressure advection is occurring over northwest Nevada. (It is important to note here that the anomalously low DT pressure values, below 200 mb, over much of northern Nevada are due to an initialization error where the convection is already occurring as seen on satellite imagery (not shown.) However, the high pressure values over west central Nevada are reasonable when compared to satellite observations at this time.) In the right panel, the DT pressure advection is computed explicitly and shows the positive values expected over northwest Nevada. Also, upward vertical motion is shown at 500 mb by the negative omega values occurring in roughly the same location. This is consistent with PV thinking.

b) Jet streaks

Vertical motion associated with jet streaks is another feature that should be analyzed especially since a maximum in wind near the tropopause (jet stream) will be associated (or induced/produced depending on your point of view) with a positive DT pressure anomaly (positive PV anomaly, Hoskins et al. 1985). Therefore, if the location of interest were to be located in a favorable region of a jet streak for upward vertical motion associated to occur, based on QG theory, while co-located with a positive DT pressure advection, the upward vertical motion would be enhanced (Figure 2.)

A second reason for looking at jet streaks has to do with the relationship between a lower DT and jet streaks mentioned above. Models may not always forecast the movement of the DT pressure anomaly accurately even 24 hours in advance (see example in Section 4), but may depict the jet streak associated with the DT pressure anomaly reasonably well. In such a case, a forecaster may be able to anticipate the possibility of a positive DT pressure anomaly also affecting the area in question. However, it would likely be done with lower confidence.

c) Gradients in moisture and/or temperature

At the surface, any pre-existing gradient in temperature and especially moisture should also be investigated. If a sharp gradient (front) were to exist in the region the DT pressure anomaly would advect over, frontogenesis (Fig. 3) will occur and will be stronger than if the gradient were weak. Thus the low-level frontogenesis will act to

enhance low-level upward motion with potentially a stronger and deeper vertical motion field extending through the troposphere.

Second, a pre-existing gradient in moisture may also indicate how close the moisture source is to the region. If the lift associated with positive pressure advection (advection of a lower DT – where the DT slopes downward) into the area were not co-located with the moisture gradient, which is often the case, the moisture gradient itself may be displaced due to the low-level response to the lift aloft. For example, consider what would happen if upward motion due to positive pressure advection on the DT were to occur to the west of a moisture boundary (Fig. 4). Beneath the area of lift, there would be an area of convergence due to mass continuity. Therefore, winds at the boundary in this case would likely have an east component with moisture advection occurring to the east of the area of lift. In this scenario, the moisture boundary would likely get pulled westward and convection may be possible further west than previously expected.

d) Instability indices including upper level lapse rates

Finally, it is also necessary to assess the thermodynamic environment of the atmosphere over the area in question to qualitatively assess the strength of the response to the forcing. Traditional stability indices, such as lifted index (LI), only look up to 500 mb so they have limited use in some of the higher elevations of the western United States. To help in assessing instability, upper level lapse rates from 500-300 mb (Fig. 5) can tell the forecaster if the atmosphere in that layer is conditionally unstable. However, using the pseudoadiabatic lapse rate of 6.5 C/km to assess conditional instability that holds true in the lower troposphere will not work in this layer due to cooler temperatures and lower water vapor saturation pressures. Therefore, it is suggested that lapse rates of 7.5 C/km be used to assess conditional instability, with a value of 8 C/km most likely to support convection.

Two other methods of assessing the instability include a 'Poor Man's Lifted Index' (PMLI, Bosart and Lackmann 1995) and a high level total totals (HLTT, Milne 2004). The PMLI uses the DT by subtracting the DT θ from the θ_e of a low-level pressure surface (in our case 700 mb since the 850 mb used in Bosart and Lackmann is often below the surface.) The net result is to get a general assessment of the conditional instability of the troposphere with values below zero being conditionally unstable (Fig. 5a). The HLTT is a modified version of the total totals index where the 700 mb level is used instead of 850 mb. Milne shows that most summer convection in the intermountain west often occurs with values of 30 C or greater. An example is shown in Fig. 5b. The major difficulty with both of these indices is that they rely on 700 mb moisture which is below mountain-top level and thus some models, particularly the Eta due to the step coordinates used, struggle with moisture advection due to lower vertical resolution in the boundary layer. Initial results show the HLTT to be of more use than the PMLI, and will be shown with the 500-300 mb lapse rates in the following section. The appendix shows how to add HLTT and PMLI to the AWIPS Volume Browser.

4. August 12, 2001 Northern Nevada dry lightning outbreak

On Aug. 12, 2001, an intense dry lightning outbreak occurred over northern Nevada into the Pacific Northwest. This outbreak will focus on northern Nevada where lightning triggered 135 new fire starts in the state with 15 being declared large (>300 acres) by 2100 PDT that evening. The following is a brief look at the Eta model forecast of the case and the RUC Analyses during the first few hours of the event which began at 09 UTC.

a) 12Z AUG 11 Eta Model Forecast for 12-18Z AUG 12

On Aug. 11, a negatively tilted short wave trough low was off the west coast, and was moving northeastward. Figures 6 and 7 show the Eta forecast for 12 UTC and 18 UTC AUG 12 respectively. The Eta shows the main circulation moving north-northeastward into Oregon and Washington by 18Z AUG 12, missing northern Nevada entirely (in the 'a' panels).

However, by looking at the Eta forecast DT pressure and 250 mb wind speed ('b' panels), the same general motion is apparent, except that the 250 mb jet streak is shown to nose into northern Nevada, especially between 12 UTC and 18 UTC AUG 12. This puts northern Nevada in a favored location for upward vertical motion from the indirect circulation of the jet streak.

The Eta also shows a pre-existing gradient in low-level θ_e lying across central Nevada, as well as 500-300 mb lapse rates exceeding 8 C/km by 12 UTC over northern Nevada, with values remaining above 7.5 C/km at 18 UTC (in the 'd' panels). However, the HLTT shows only values of 20-25 C over northwest Nevada with values over 30 C in much of eastern Oregon. Thus, even though it appears that the main circulation center is moving into Oregon and Washington, northern Nevada may have convection due to steep upper level lapse rates, but at this time it appears isolated.

b) RUC Analyses of the event

The RUC analysis for the event shows the main positive DT pressure center off the northern California coast with a weak lobe extending into central Nevada (Fig. 8) by 06 UTC 12 Aug. The DT pressure lobe then continues northward through northern Nevada while the PV center moves into Oregon by 18 UTC (Fig. 10) as the Eta forecast depicted. It is apparent that upward vertical motion should occur ahead of the DT pressure lobe over northern Nevada, which was not forecast by the Eta (Fig. 6 & 7).

The RUC analysis in Figure 8 also shows the 250 mb jet streak on the south side of the anomaly is also in a favorable location for upward vertical motion, especially at 06 and 12 UTC. Both the positive DT pressure anomaly and its associated jet streak will work in tandem in this case to bring about stronger upward vertical motion than would be otherwise expected, if only one were present.

As for the θ_e gradient (Figs. 8, 9, 10), it is apparent in the RUC analyses that the gradient is further west than the Eta forecast due to the low level convergence occurring underneath the upward motion in maintaining mass continuity. This is especially true at 12 and 18 UTC. In addition, the atmosphere is even more unstable than forecast by the Eta as the 500-300 mb lapse rates in the RUC Analyses are greater than 8 C/km over northern Nevada from 06-12 UTC. The HLTT verified the greater instability as well and the Eta did not forecast the low level moisture advection well. Although values of 20-25 C over northwest Nevada were accurately depicted until 12 UTC, by 18 UTC values of 30 C or greater were present across almost all of Nevada indicating a greater potential for convection.

A lightning plot during the peak of the event is shown in Figure 11. It shows the intense amount of lightning observed over Nevada for one hour ending at 20 UTC with over 1500 strikes.

Also of interest in this case, and was mentioned in Section 3, is that although the upper level feature itself may not be accurately forecast, if the meteorologist understands the link between jet streaks and positive DT pressure anomalies, an adjustment can be made in such situations, including Aug. 12, 2001. Thus, a jet streak moving into an area will indicate the possible location for an upper level front, even if the model does not bring the upper level feature itself into the area.

5. Summary

The use of DT plots versus isentropic and/or pressure layer charts allows the meteorologist to better understand the three dimensional aspects of an upper level disturbance on a two-dimensional display. When used in conjunction with locations for favored jet streak forcing, pre-existing boundaries, and an assessment of upper level conditional instability, the DT plots will better equip the knowledgeable forecaster to predict dry thunderstorm events, especially with respect to negatively tilted short wave troughs.

A brief case study of the 12 Aug 2001 northern Nevada dry lightning bust was also presented and illustrated two important points. One, occasionally the jet streaks associated with an upper level positive DT pressure anomaly are better forecast than any lobes of the DT anomaly itself. Two, the high level lapse rates are the best of the instability methods presented to show possible convection with conditionally unstable lapse rates. However, the HLTT also shows some potential towards forecasting instability provided the model forecasts the low level moisture advection reasonably well, but is probably best used as a nowcasting tool to verify the potential for convection during a possible event.

Acknowledgements. I would like to thank Chris Gibson, NWSFO Salt Lake City and Greg Mann, NWSFO White Lake, MI for their brief but informative discussions on potential vorticity and the dynamic tropopause. In addition, I would like to thank Rhett Milne and Mark Mollner for their comments and review of the paper.

Appendix

Adding Poor Man's Lifted Index and High Level Total Totals to AWIPS

In order to get PMLI and HLTT into the volume browser on AWIPS, you (or your IT or AWIPS focal point) will need to edit a couple files in the '/dsdata/customFiles' directory. The following is a list of the files that need to be changed and the lines that WFO Reno has added for both PMLI and HLTT (case sensitive – file names in italics).

PMLI

virtualFieldTable.txt

```
poorLI  |  |  N  |  Poor Mans LI  | K   |  CONTOUR,IMAGE |  | \
        *Difference,Layer| PoT,Trop | EPT,700MB
```

contourStyle.rules

```
* poorLI,Layer
        |  1  |  0  |  2  |  |  |xn| 8000F0FF |  |  0  |  2
```

gridImageStyle.rules

```
* poorLI,Layer
        |  1  |  0  |  0  |  30  |  |  |  29  |  0  |  5
```

HLTT

virtualFieldTable.txt

```
modtt  |  |  N  |  Modified tTotals | C  |  CONTOUR,IMAGE |  | \
        *LinTrans,Layer | 1.0 | T,700MB | 1.0 | DpT,700MB| 2.0 | T,500MB
```

contourStyle.rules

```
* modtt,Layer
        |  1  |  0  |  4  |  |  |..| 8000F0FF |  |  0  |  2
```

gridImageStyle.rules

```
* modtt,Layer
        |  1  |  0  |  0  |  50  |  |  |  29  |  0  |  4
```

REFERENCES

Bluestein, H., 1993. *Synoptic-Dynamic Meteorology in Midlatitudes. Vol II: Observations and Theory of Weather Systems.* Oxford University Press. 594 pp.

Bosart, L. F., and G. M. Lackmann, 1995: Postlandfall Tropical Cyclone Reintensification in a Weakly Baroclinic Environment: A Case Sstudy of Hurricane David (September 1979). *Mon. Wea. Rev.*, **123,** 3268-3291.

____, G. J. Hakim, K. R. Tyle, M. A. Bedrick, W. E. Bracken, M. J. Dickinson, and D. M. Schultz, 1996: Large-scale Antecedent Cconditions Associated with the 12-14 March 1993 Cyclone ("Superstorm '93") over eastern North America. *Mon. Wea. Rev.*, **124,** 1865-1891.

Hakim, G., L. F. Bosart, and D. Keyser, 1995: The Ohio Valley Wavemerger Cyclogenesis Event of 25-26 January 1978. Part II: Diagnosis Using Quasigeostrophic Potential Vorticity Inversion. *Mon. Wea. Rev.* **124,** 2176-2205.

Gibson, C. V., 1995. Operational Use of Potential Vorticity to Identify the Location, Strength and Movement of Upper-level Fronts. *Western Region Technical Attachment No. 95-15,* May 16,1995.

____, 1996. Using Isentropic Potential Vorticity in Forecasting the Intensity of Frontal Boundaries: Case Study of the Cold Front Affecting the South Canyon Fire. Preprints, *First Symposium on Fire and Forest Meteorology.*

Hirschberg, P. A. and J. M. Fristch, 1991a. Tropopause Undulations and the Development of Extratropical Cyclones. Part I: Overview and Observations from a Cyclone Event. *MWR,* **119,** 496-517.

____, and J. M. Fristch, 1991b. Tropopause Undulations and the Development of Extratropical Cyclones. Part II: Diagnostic Analysis and Conceptual Model. *MWR,* **119,** 518-550.

Holton, J. R., 1992. An Introduction to Dynamic Meteorology. Academic Press, New York, New York, 511 pp.

Hoskins, B., M. McIntyre, and A. Robertson, 1985: On the Use and Significance of Isentropic Potential Vorticity Maps. *Quart. J. Roy. Meteor. Soc.*, **111,** 877-946.

____, and P. Berrisford, 1988: A Potential Vorticity Perspective of the Storm of 15-16 October '87. *Weather,* **43,** 122-129.

Milne, R., 2004. A Modified Total Totals Index for Thunderstorm Potential over the Intermountain West. *WR Technical Attachment No. 04-04.*

National Weather Service, 1996. Critical Fire Weather Patterns of the Western United States. *Material from the National Fire Weather Forecasters Course*.

Rorig, M. L., and S. A. Ferguson, 1999: Characteristics of Lightning and Wildland Fire Ignition in the Pacific Northwest. *J. Appl. Meteor.*, **103,** 1565-1575.

____, S. A. Ferguson and S. McKay, 2003: Forecasting Dry Lghtning in the western United States. Preprints, *Fifth Symposium on Fire and Forest Meteorology*.

Shapiro, M. A., and E. D. Grell, 1994: In Search of Synoptic/Dynamic Conceptualizations of the Life Cycles of Fronts, Jet Streams and the Tropopause. *The Life Cycles of Extratropical Cyclones,* Vol. I. S. Gronas and M. A. Shapiro, Eds., Aase Grafiske A/S, 163-181.

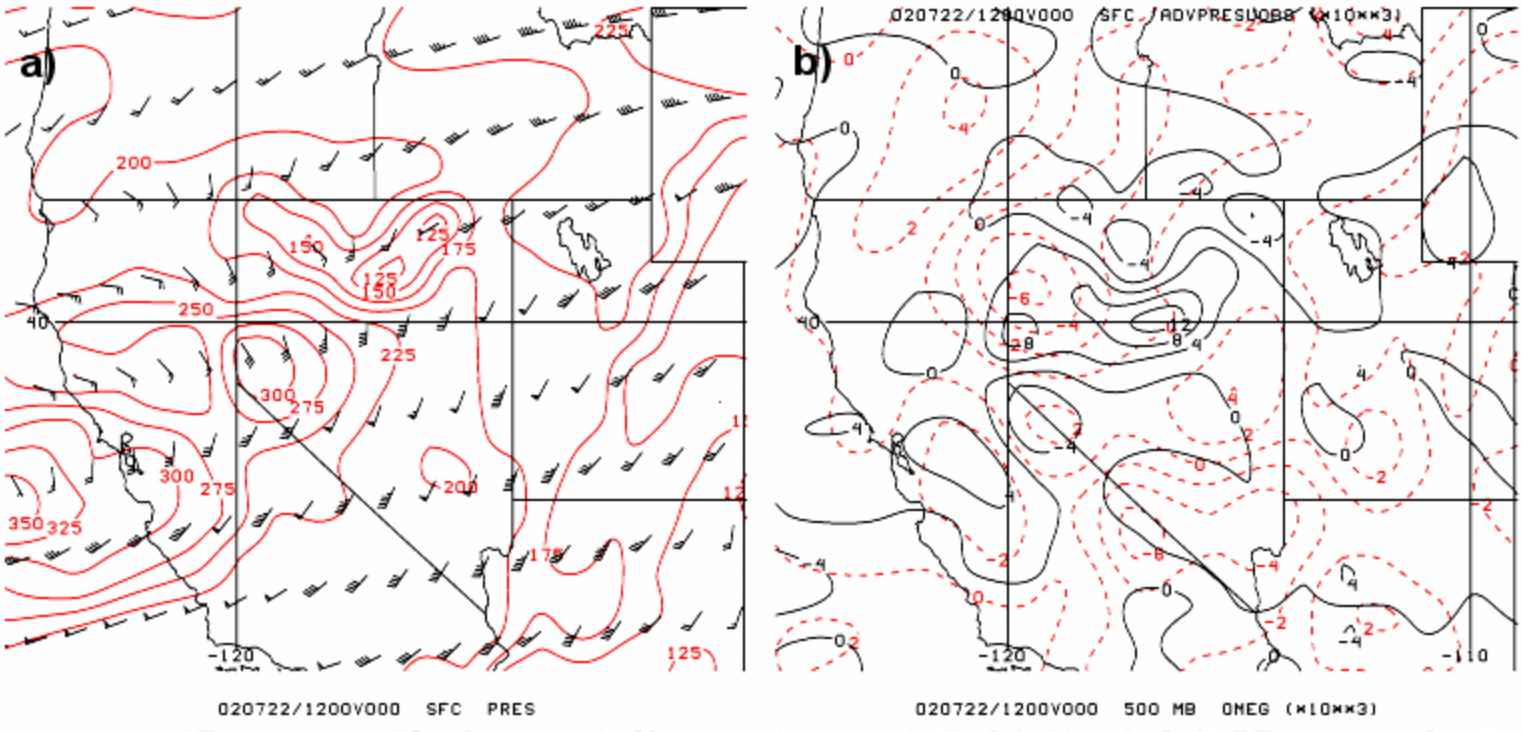

Figure 1. 12 UTC RUC Analysis for 22 Jul 2002. a) DT pressure (solid red, mb) and wind (full barb is 10 kts). In b) DT pressure advection (solid black, 10^{-3} mb/s) and 500 mb omega (dashed red, μb/s).

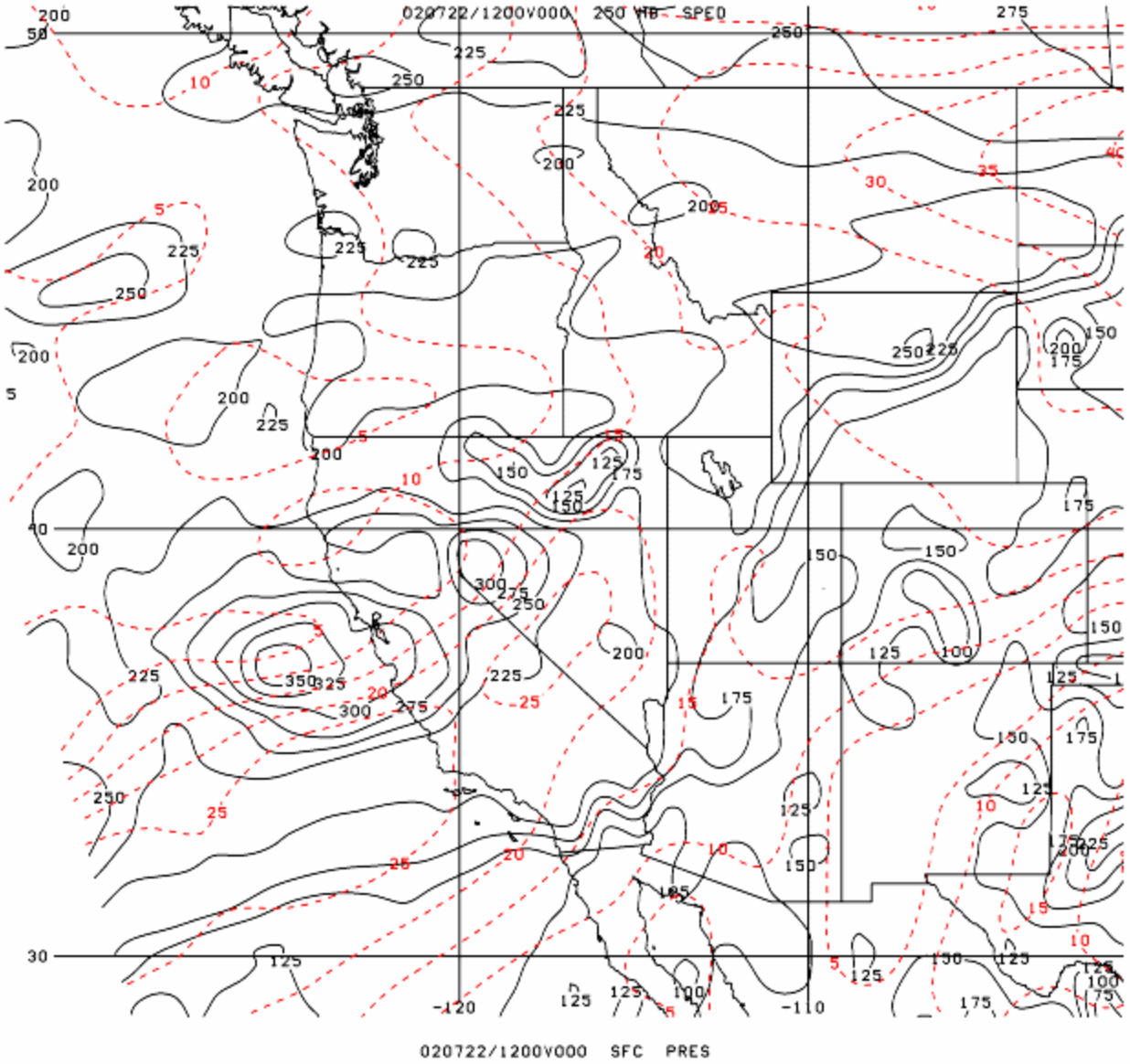

Figure 2. 12 UTC RUC Analysis for 22 Jul 2002 with DT pressure (solid black, mb) and 250 mb wind speed (dashed red, m/s).

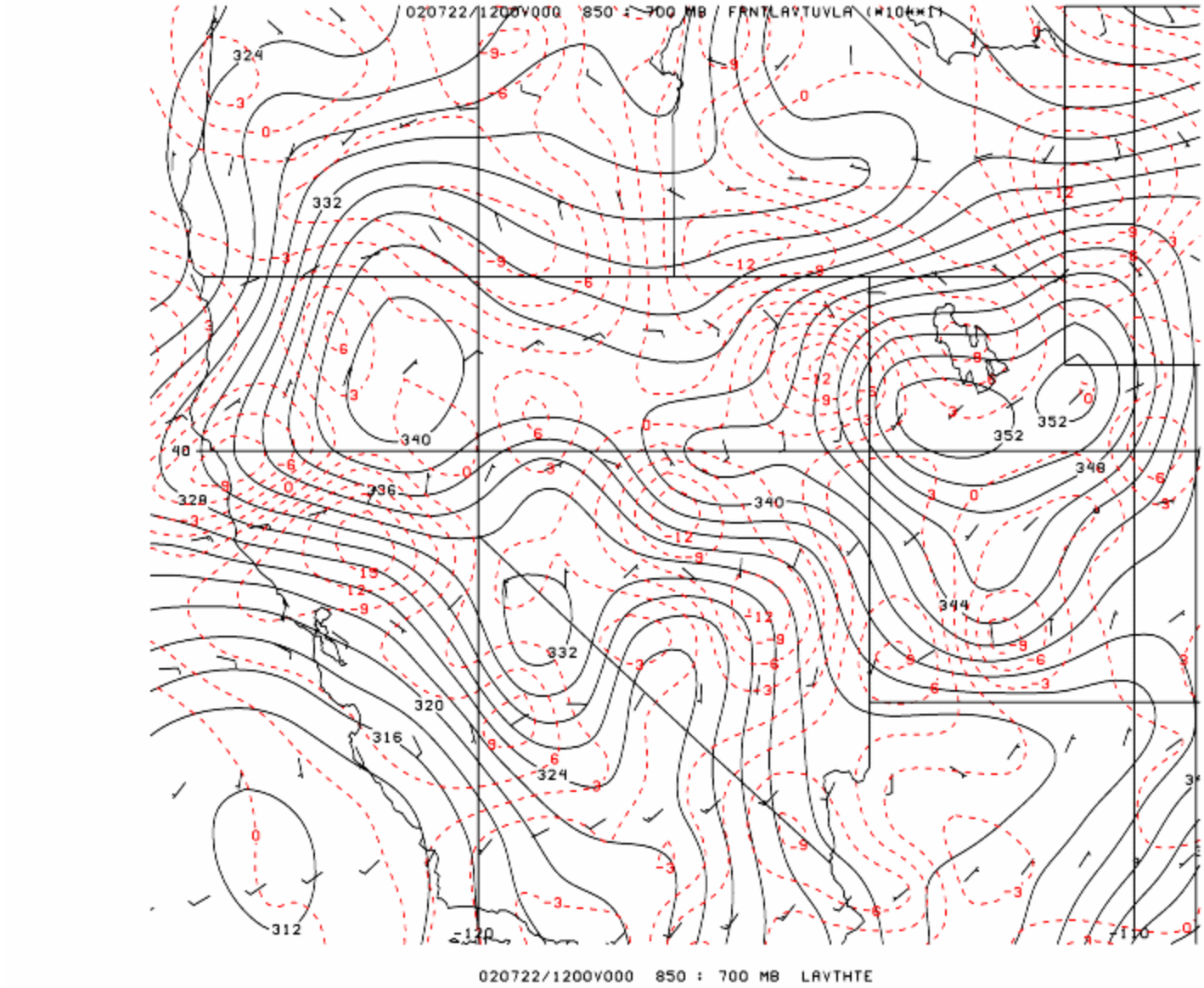

Figure 3. 12 UTC RUC Analysis for 22 Jul 2002. 850-700 mb θ_e (solid black, K) and θ_e frontogenesis (dashed red, 10^1 K/12 hr).

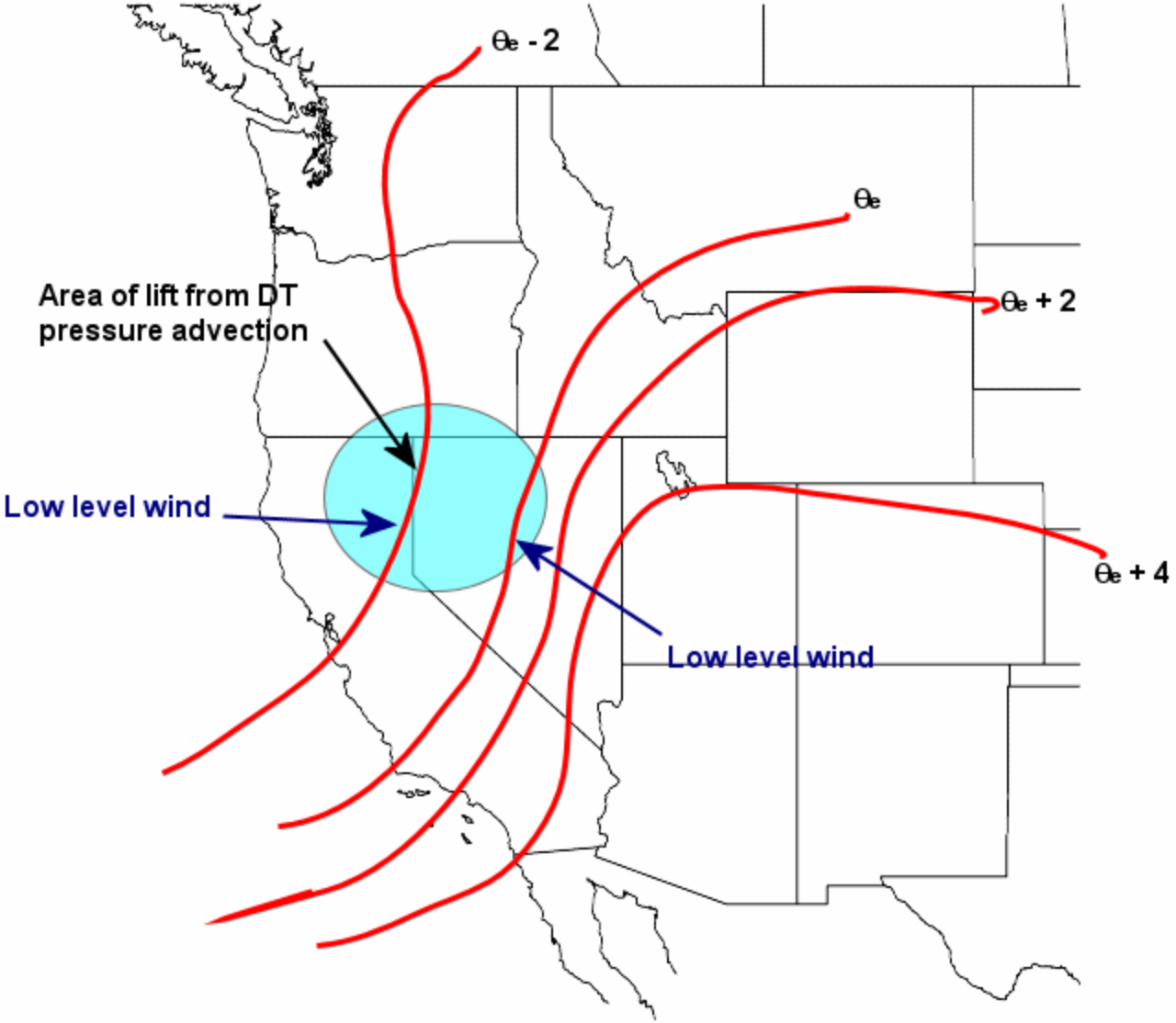

Figure 4. Schematic showing the potential effect on a low-level θ_e gradient when the lift and low-level convergence associated with positive DT pressure advection is west of the gradient.

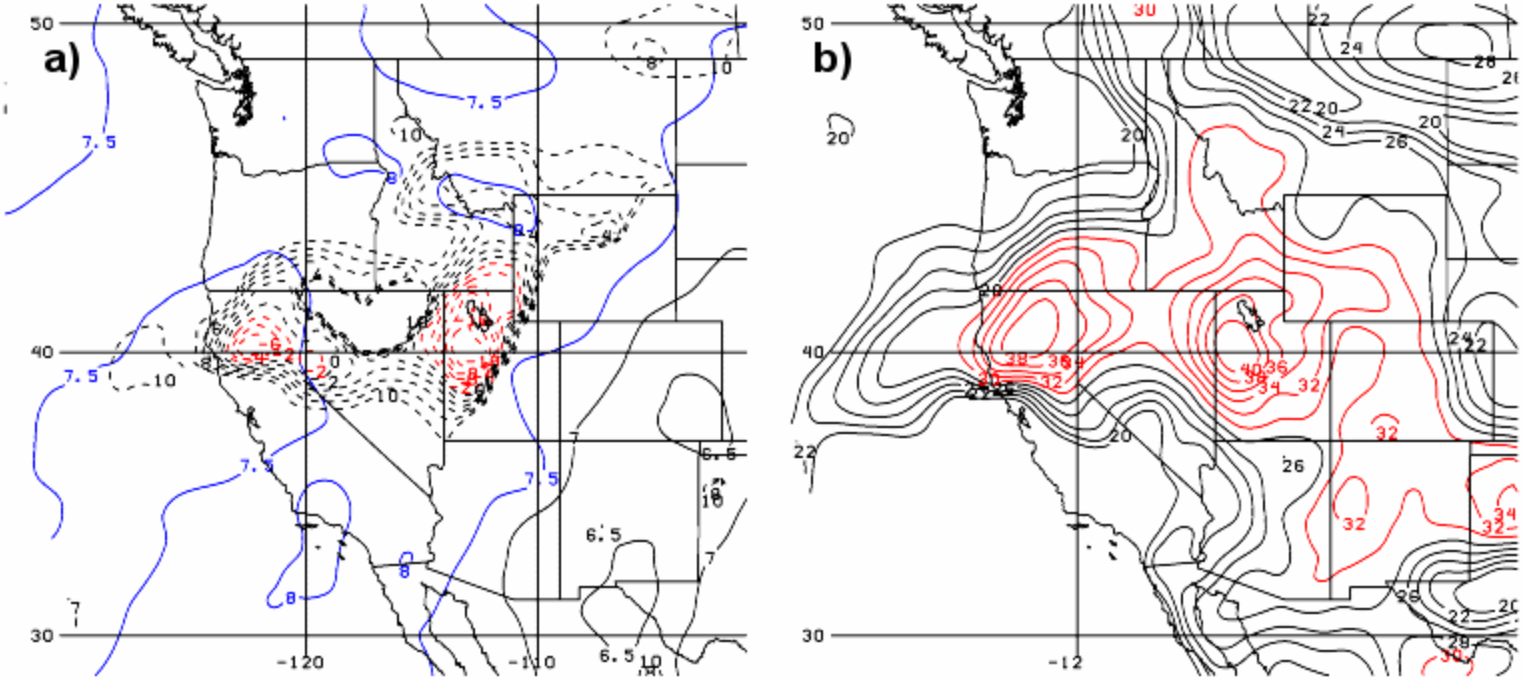

Figure 5. 12 UTC RUC Analysis for 22 Jul 2002. a) PMLI (dashed contours from -10 to 10 C with values less than zero in red) and 500-300 mb lapse rate (solid, with values of 7.5 C or greater in blue). b) HLTT (solid with values 30 C or greater in red).

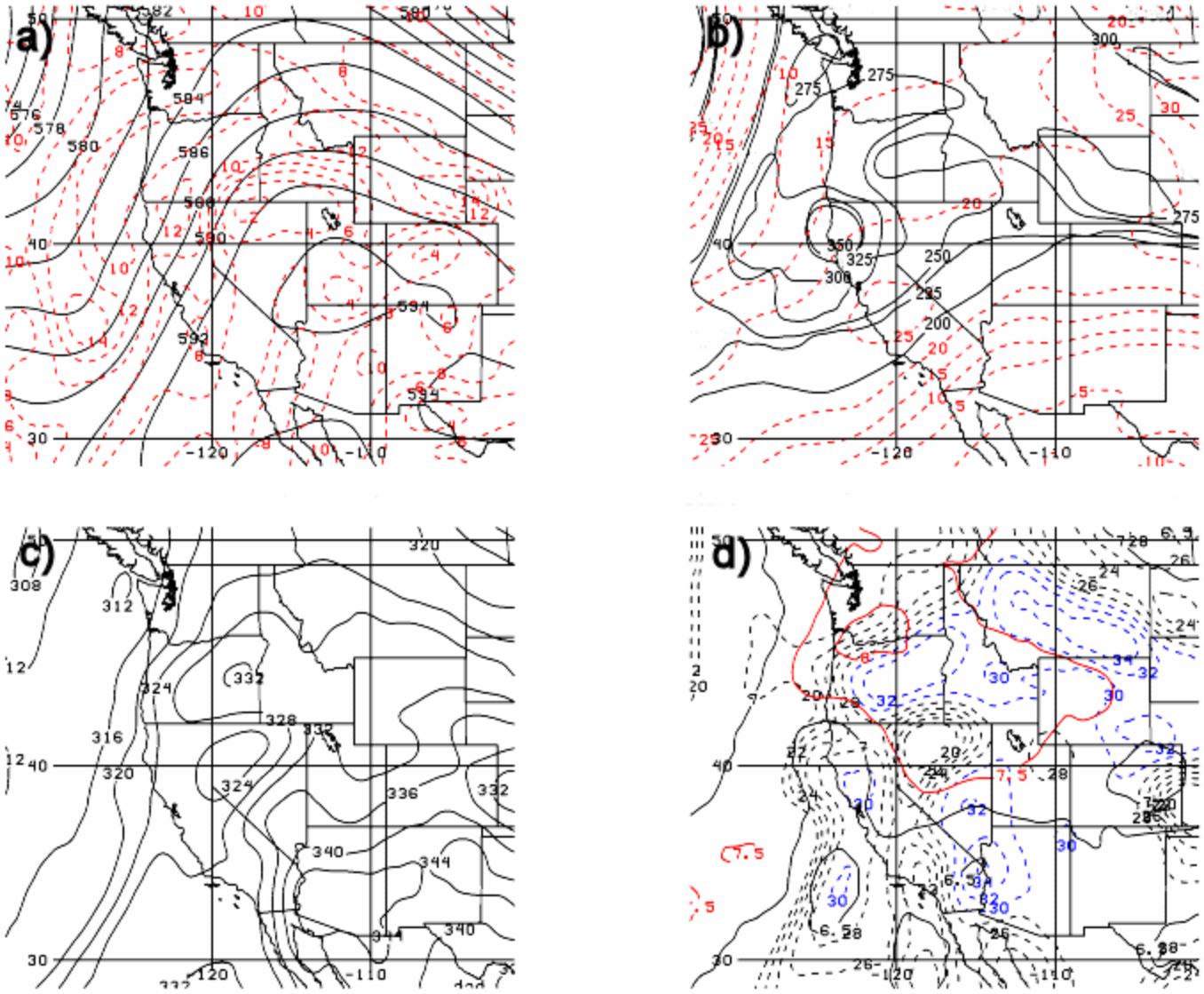

Figure 6. 11 Aug 2001 12 UTC Eta 24 hr forecast for 12 UTC 12 Aug. a) 500 mb heights (solid black, Dm) and vorticity (dashed red, s^{-1}). b) DT pressure (solid black, mb) and 250 mb wind speed (dashed red, m/s). c) 850-700 mb θ_e (K) and d) 500-300 mb lapse rate (solid, with values of 7.5 C or greater in red) and HLTT (dashed with values 30 C or greater in blue).

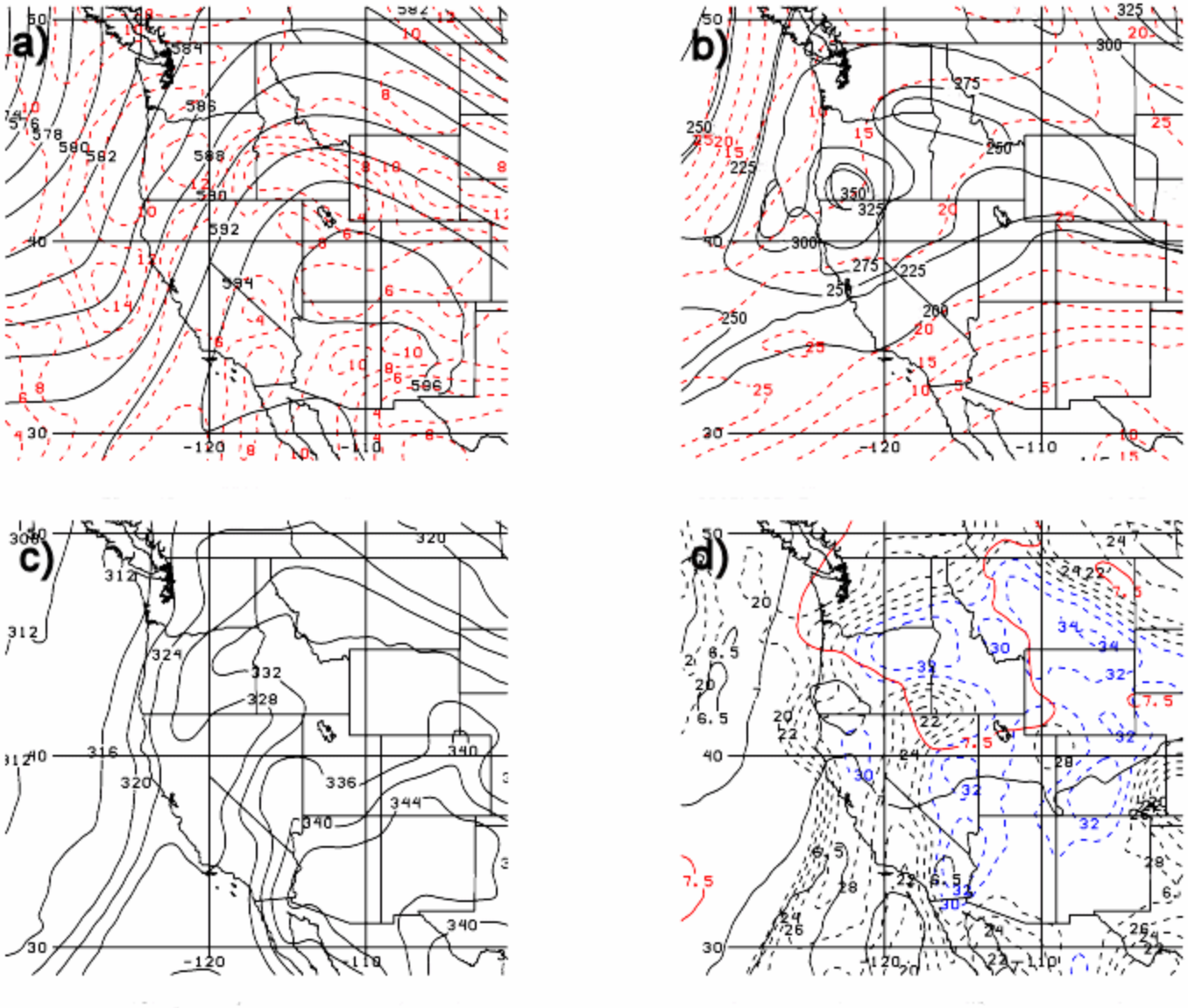

Figure 7. Same as in Fig. 6 except 30 hr Eta forecast for 18 UTC 12 Aug.

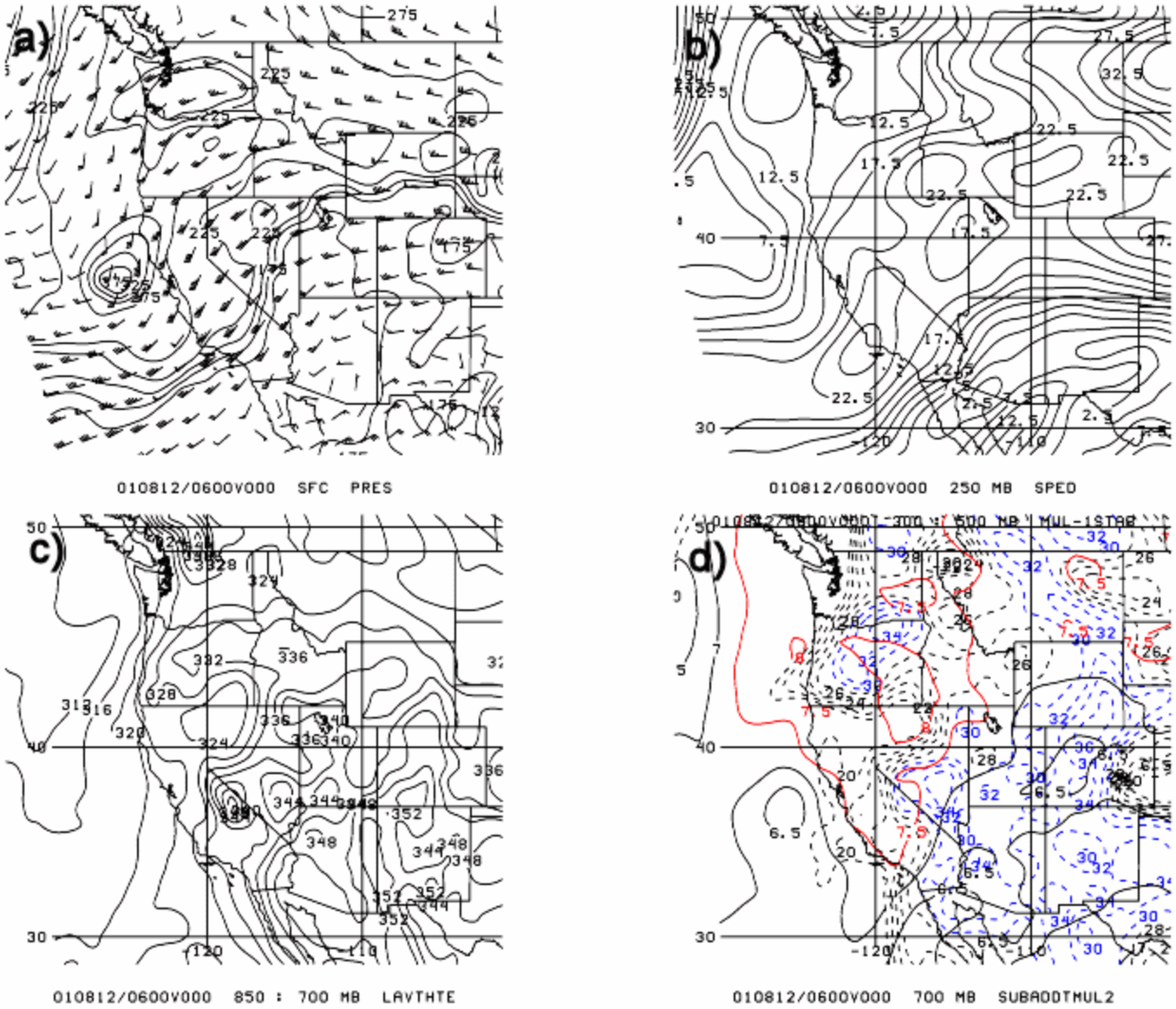

Fig. 8. 06 UTC RUC Analysis for 12 Aug 2001. a) DT pressure (mb) and wind (full barb is 10 kts). b) 250 mb wind speed (m/s). c) 850-700 mb θ_e (K) and d) 500-300 mb lapse rate (solid, with values of 7.5 C or greater in red) and HLTT (dashed with values 30 C or greater in blue).

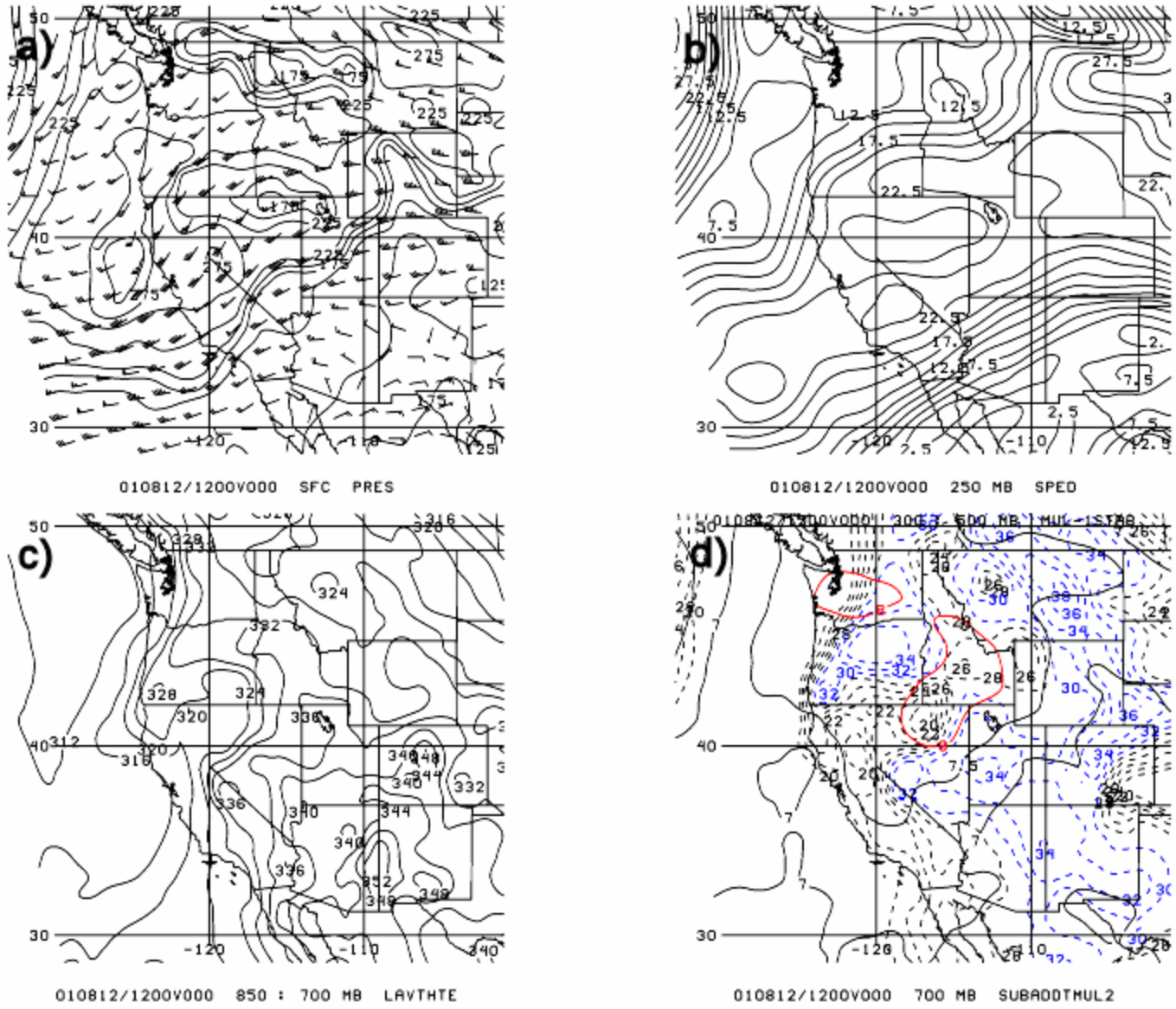

Figure 9. Same as in Fig. 8 except for the 12 UTC RUC Analysis on 12 Aug 2001.

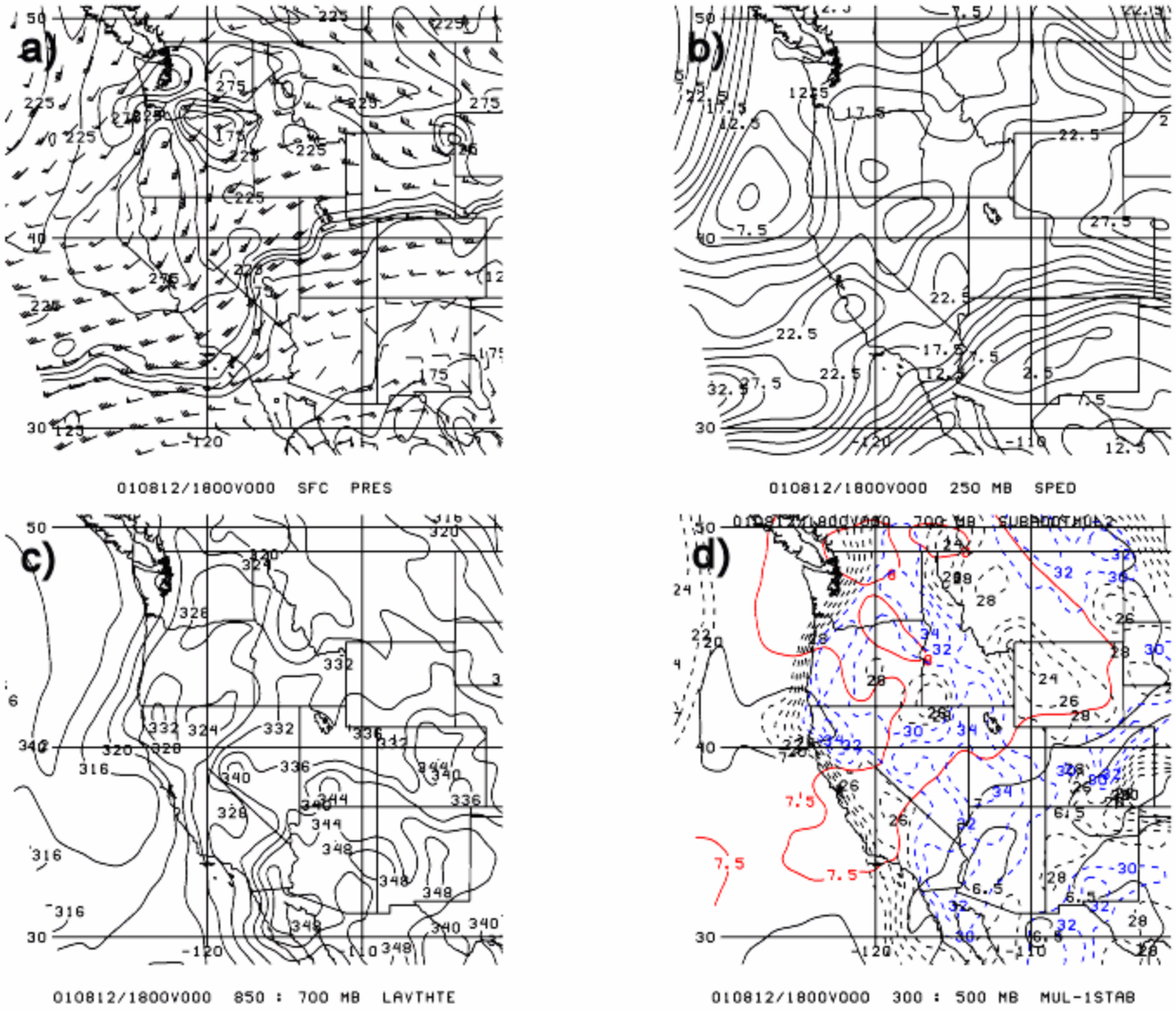

Figure 10. Same as in Fig. 8 except for the 18 UTC RUC Analysis on 12 Aug 2001.

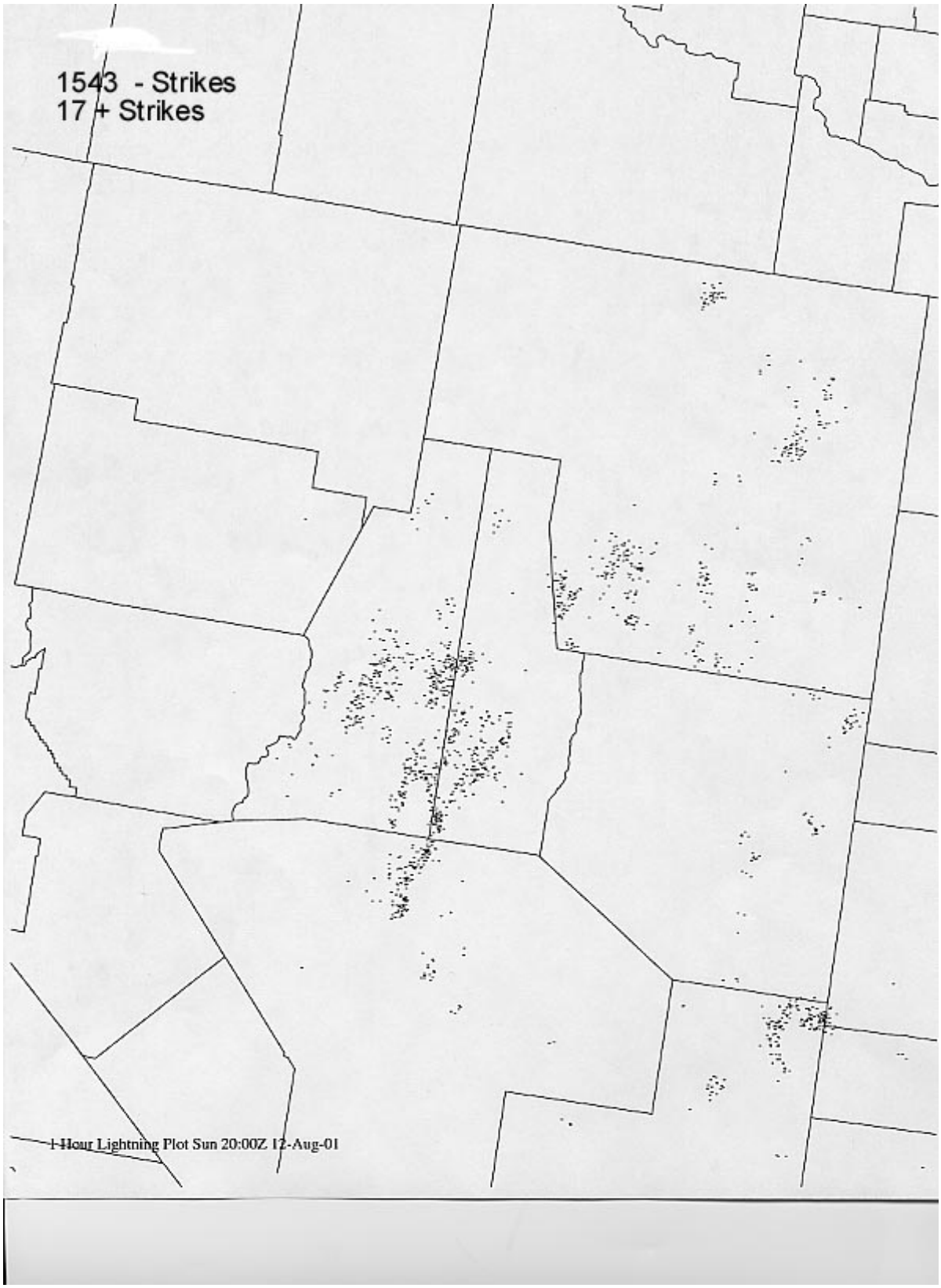

Figure 11. One hour lightning plot ending at 20 UTC 12 Aug 2001.